Multivalency Amplifies the Selection and Affinity of Bradykinin-Derived Peptide for Lipid Nanovesicles

Jonel P. Saludes,[a,b] Leslie A. Morton,[a] Sara K. Coulup,[a] Zeno Fiorini,[a] Brandan M. Cook,[b] Lida Beninson,[c] Edwin R. Chapman,[d] Monika Fleshner,[c] and Hang Yin[a]

[a]Department of Chemistry & Biochemistry and BioFrontiers Institute, University of Colorado, Boulder, CO 80309, U.S.A. [b]Department of Chemistry, Washington State University, Pullman, WA 99164, U.S.A. [c]Department of Integrative Physiology, University of Colorado, Boulder, CO 80309, U.S.A. [d]Howard Hughes Medical Institute and Department of Neuroscience, University of Wisconsin, Madison, WI 53706, U.S.A.

Email: hang.yin@colorado.edu

Supporting Information

TABLE OF CONTENTS

Page

A. Synthesis and Characterization

A.1. Solid Phase Peptide Syntheses.

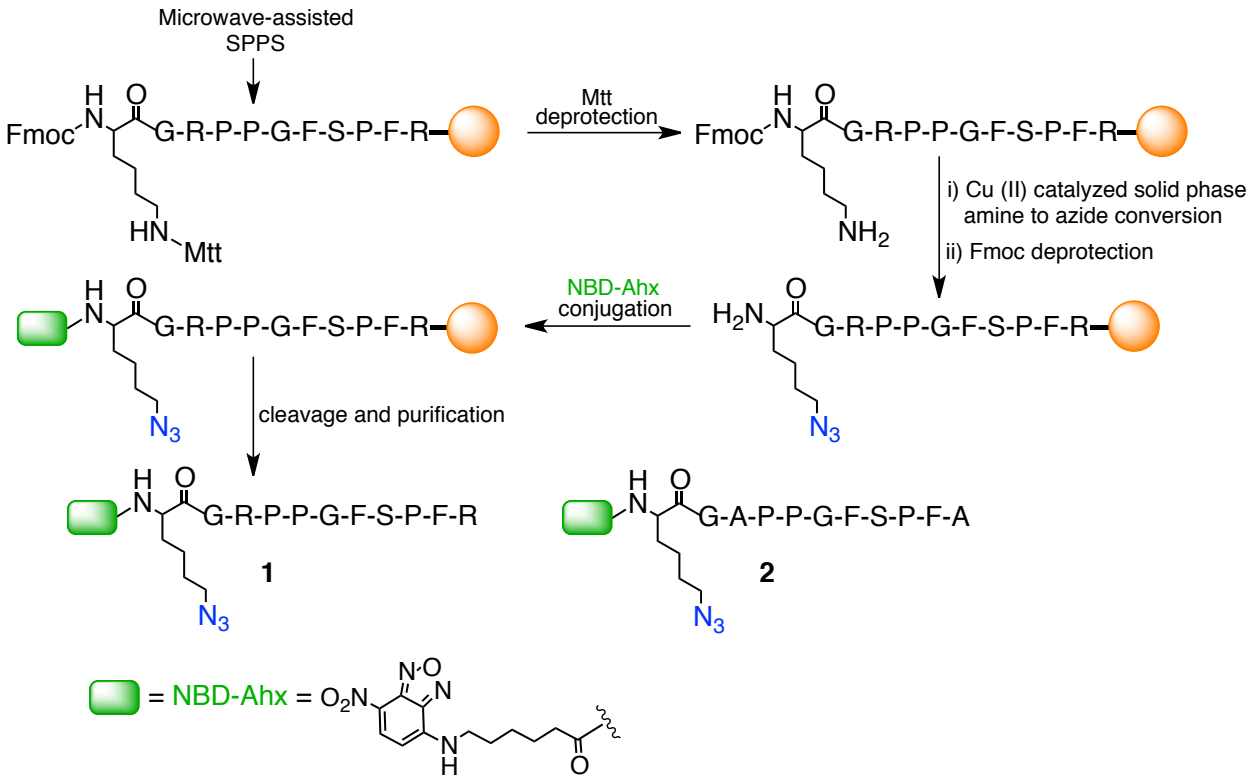

Peptide Resin-**1a** [Fmoc-K(Mtt)GRPPGFSPFR] was synthesized using either Liberty (CEM, Matthews, North Carolina) or Biotage Initiator+ SP Wave (Charlotte, North Carolina) microwave-assisted solid phase peptide synthesizer following the standard Fmoc chemistry. Rink amide resin and all reagents were purchased from commercial sources and used as received. Typically, 0.1 mmol of Rink amide MBHA resin (loading capacity = 0.67 mmol g^{-1}) and 5 equiv. each of the Fmoc-protected amino acids (0.5 mmol), HBTU (0.5 mmol), and DIPEA (0.5 mmol) in 4 mL DMF were used for the coupling step. Reaction conditions were as follows: power = 25 W, hold time = 5 min, temperature = 75 °C. Fmoc deprotection required 7 mL of 5% piperazine and 0.1 M HOBt in DMF. All coupling and deprotection processes were repeated to ensure complete loading and deprotection. To selectively remove the Mtt-protection of the ε-amino group of peptide Resin-**1a**, 0.09 mmol of the resin-bound peptide was treated with

94% CH_2Cl_2, 1% TFA, and 5% triisopropylsilane (TIPS) (10 mL x 3 min x 10) at r.t., followed by thorough washing with CH_2Cl_2 and MeOH (5 mL x 3). The completion of Mtt deprotection was tested by Kaiser test and was confirmed when the resin turned purple in color. After deprotection, the resin was swelled in a mixture of 560 μL CH_2Cl_2, 520 μL MeOH, 490 μL H_2O, and 2 μL Et_3N for 2 h, drained, and treated with $CuSO_4$ (2.7 mg, 0.018 mmol, in 30 μL H_2O,) and freshly prepared TfN_3 (3.6 mmol in 5.5 mL CH_2Cl_2).[1] The mixture was stirred for 24 h at r.t., followed by washing with MeCN, DMF, H_2O, 0.1 M EDTA, H_2O, MeOH, CH_2Cl_2, and MeOH. Kaiser test and FT-IR spectroscopic analysis were performed to confirm the conversion of NH_2 to N_3. The *N*-terminus was deprotected using 5 mL of 20% piperidine in 1-Methyl-2-pyrrolidinone (NMP) and fluorescently labeled using 44.25 mg (0.15 mmol) of NBD-Ahx (Anaspec, Fremont, CA) and HATU (57 mg, 0.15mmol). The peptide was washed with 5 mL each of DMF, CH_2Cl_2, and MeOH (x3), cleaved from the resin using 10 mL of 85/5/5/5 TFA/H_2O/phenol/TIPS, purified by reverse phase HPLC using a 10 x 250 mm C18 column (Phenomenex Synergi, Torrance, California), and lyophilized to dryness to yield peptide **1** (BKKG). Peptide **2** (BKKG-R3AR11A) was prepared in the same manner as described for **1**. Both peptides were characterized by MALDI-TOF-MS (Applied Biosystems Voyager, Carlsbad, California): BKKG **1**, $[M+H]^+$ calculated for $C_{70}H_{100}N_{25}O_{16}^+$, 1546.8; found, 1547.2; $[M+Na]^+$ calculated for $C_{70}H_{99}NaN_{25}O_{16}^+$, 1569.2; found, 1315.5; BKKG-R3AR11A **2**, $[M+Na]^+$ calculated for $C_{64}H_{85}N_{19}NaO_{16}^+$, 1398.6; found, 1398.3; $[M+K]^+$ calculated for $C_{64}H_{85}KN_{19}O_{16}^+$, 1414.6; found, 1414.3. ^1H NMR spectra were also recorded using a 500 or 600 MHz spectrometer (Varian, Palo Alto, California) at 293 K in 9:1 H_2O/D_2O (referenced to HDO, δ_H = 4.79) as additional characterization.

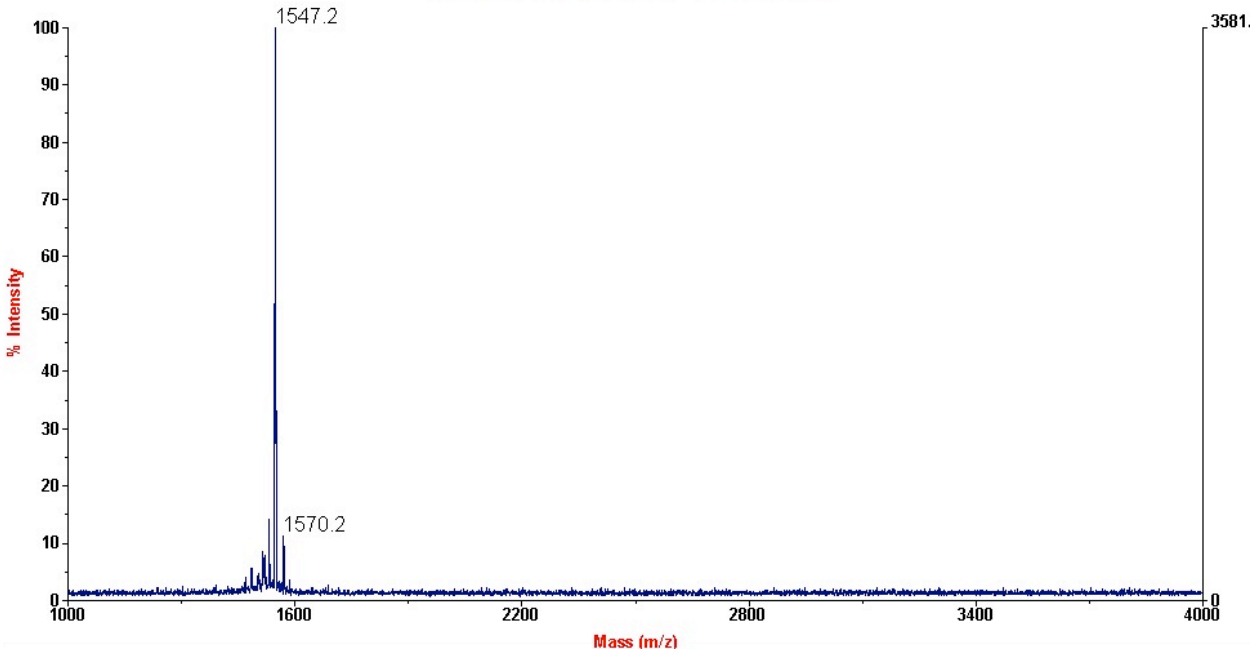

Figure S1. MALDI-TOF-MS of BKKG **1**.

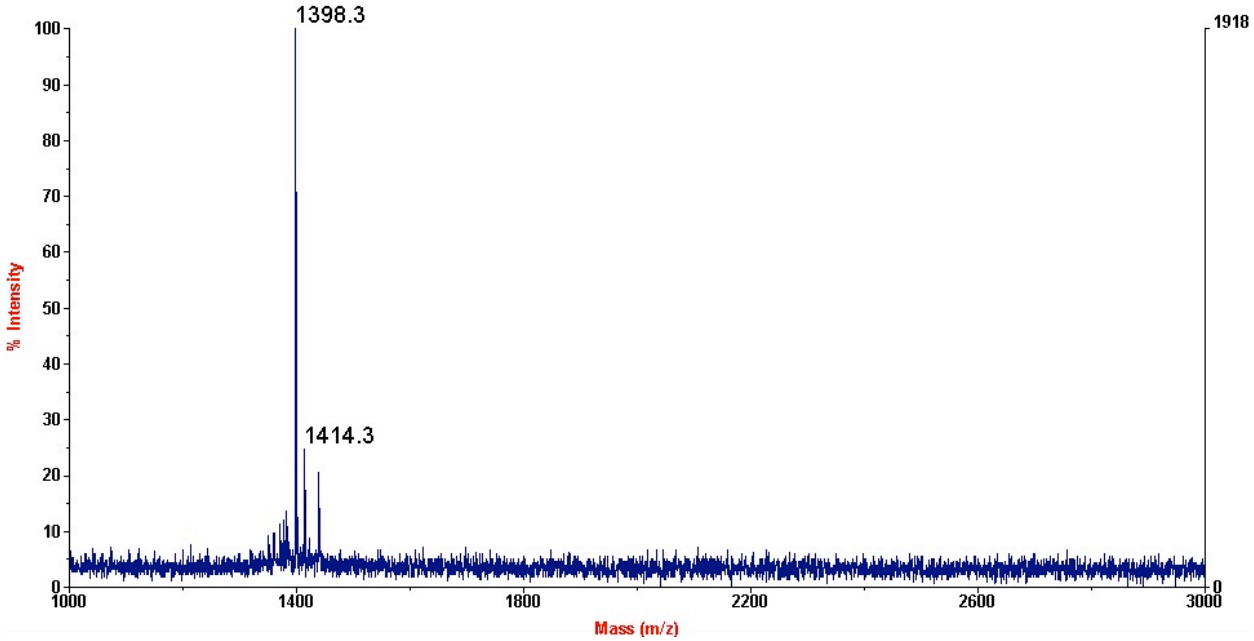

Figure S2. MALDI-TOF-MS of BKKG-R3AR11A **2**.

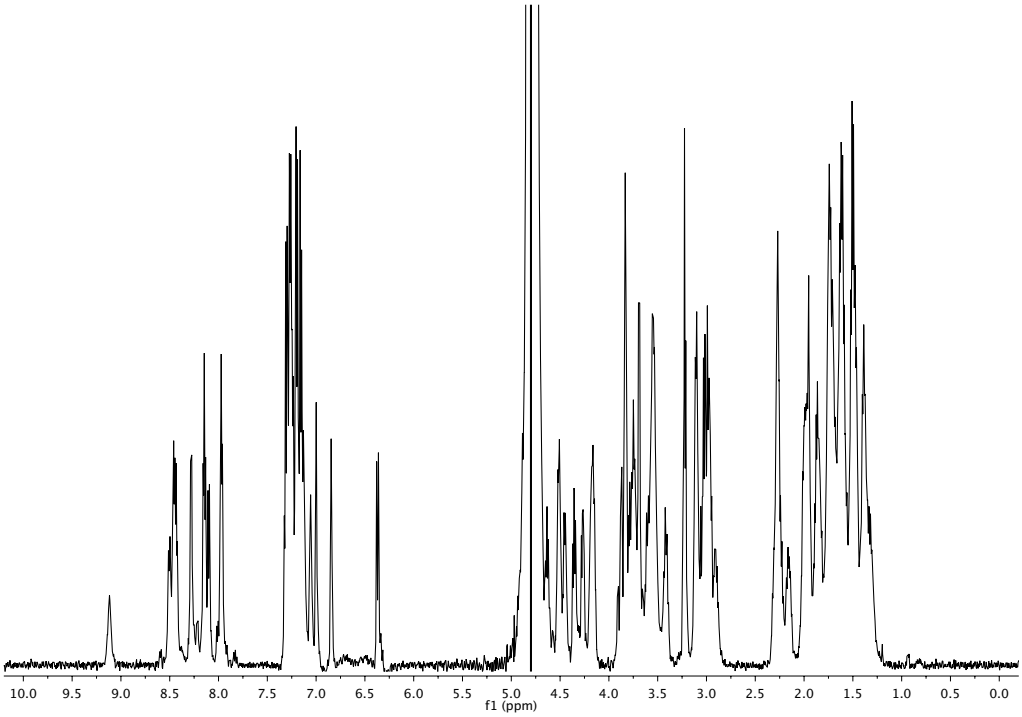

Figure S3. ^{1}H NMR spectrum of BKKG **1** in 9:1 H_2O/D_2O, 500 MHz, 293 K.

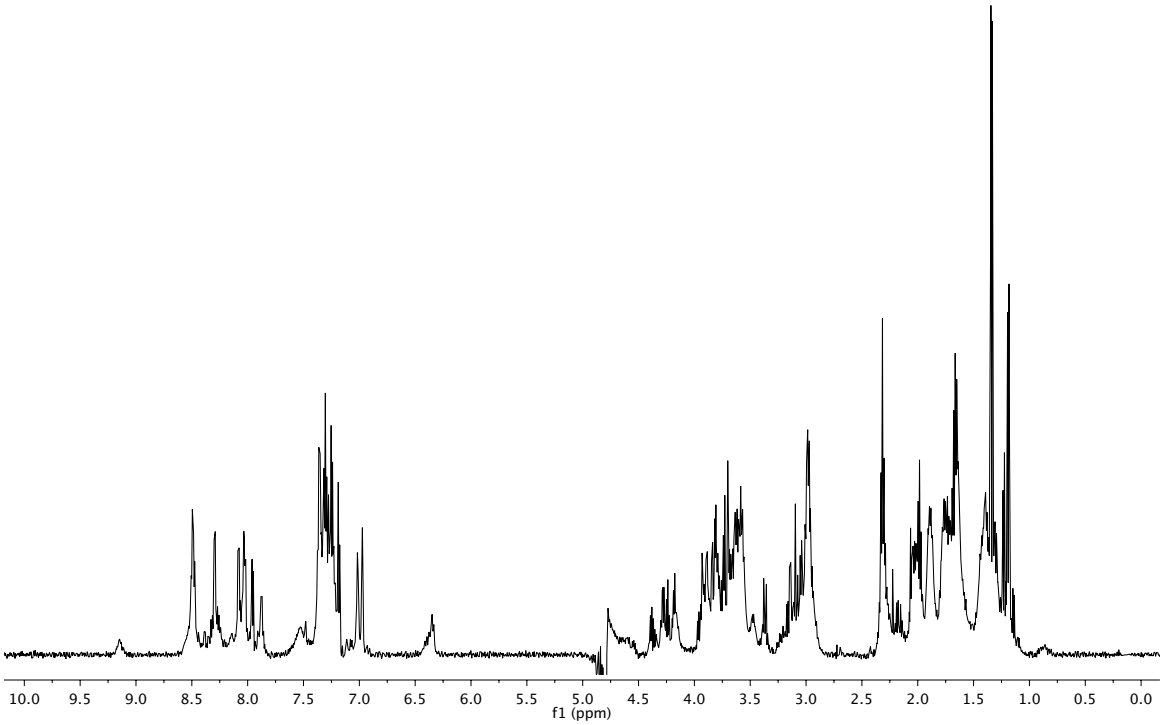

Figure S4. ^{1}H NMR spectrum of BKKG-R3AR11A **2** in 9:1 H_2O/D_2O, 600 MHz, 293 K.

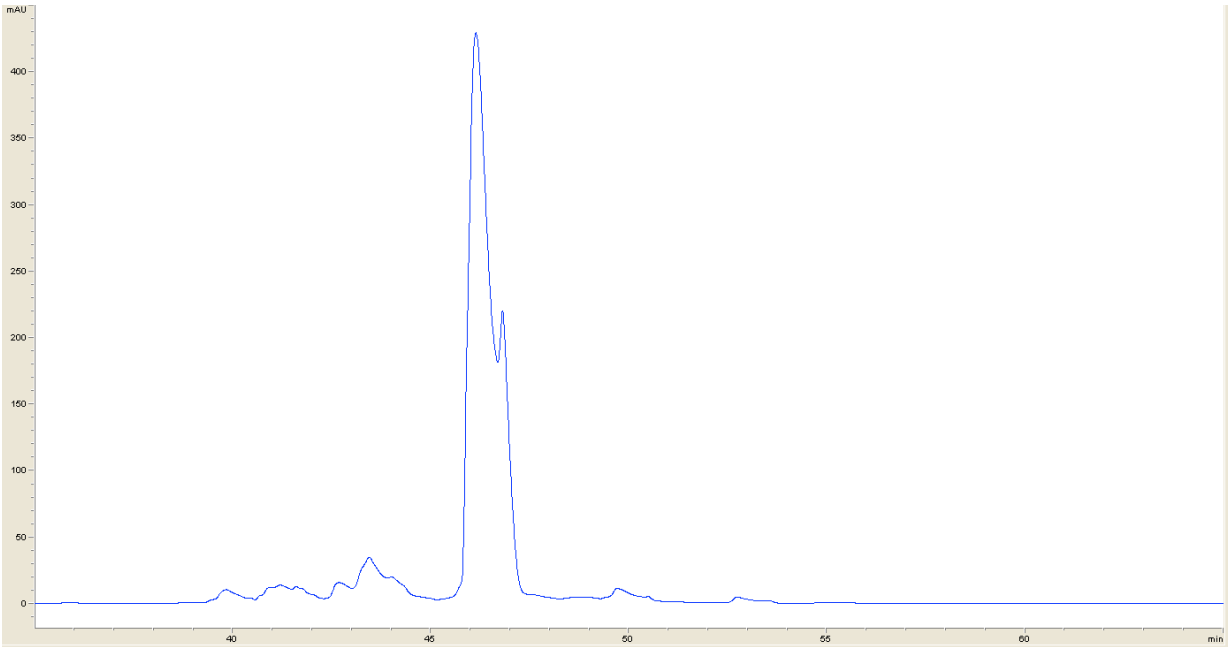

Figure S5. HPLC trace of BKKG **1**.

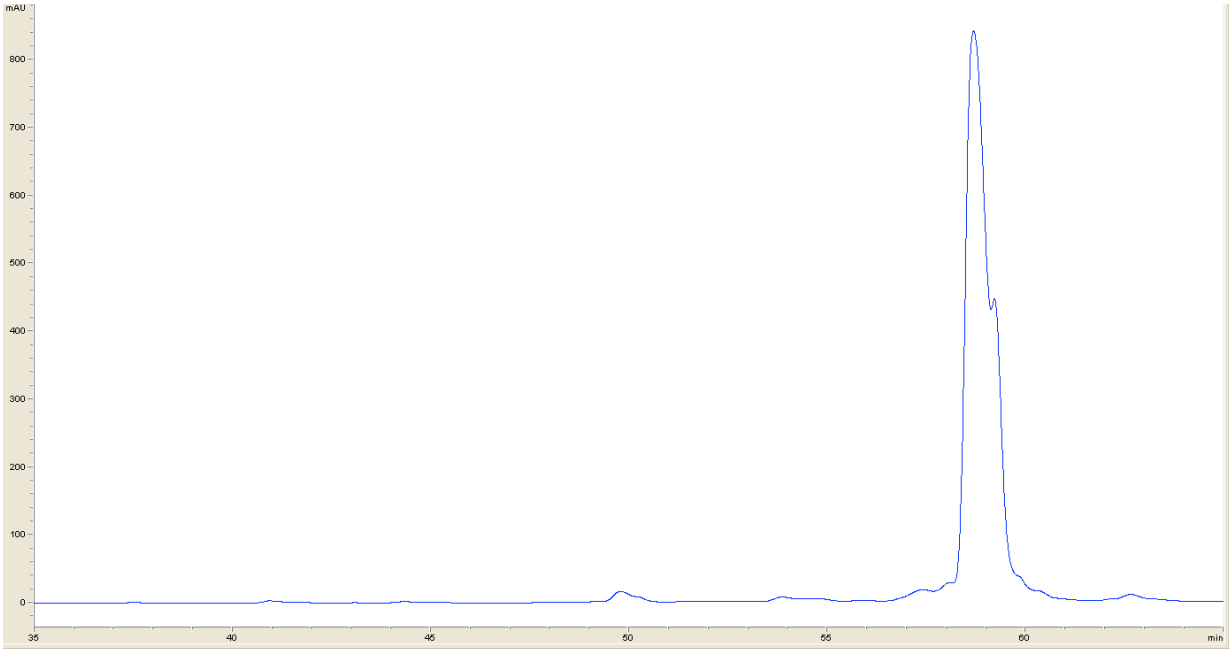

Figure S6. HPLC trace of BKKG-R3AR11A **2**.

A.2. Trimer Synthesis by Solution Phase 'Click' Chemistry.

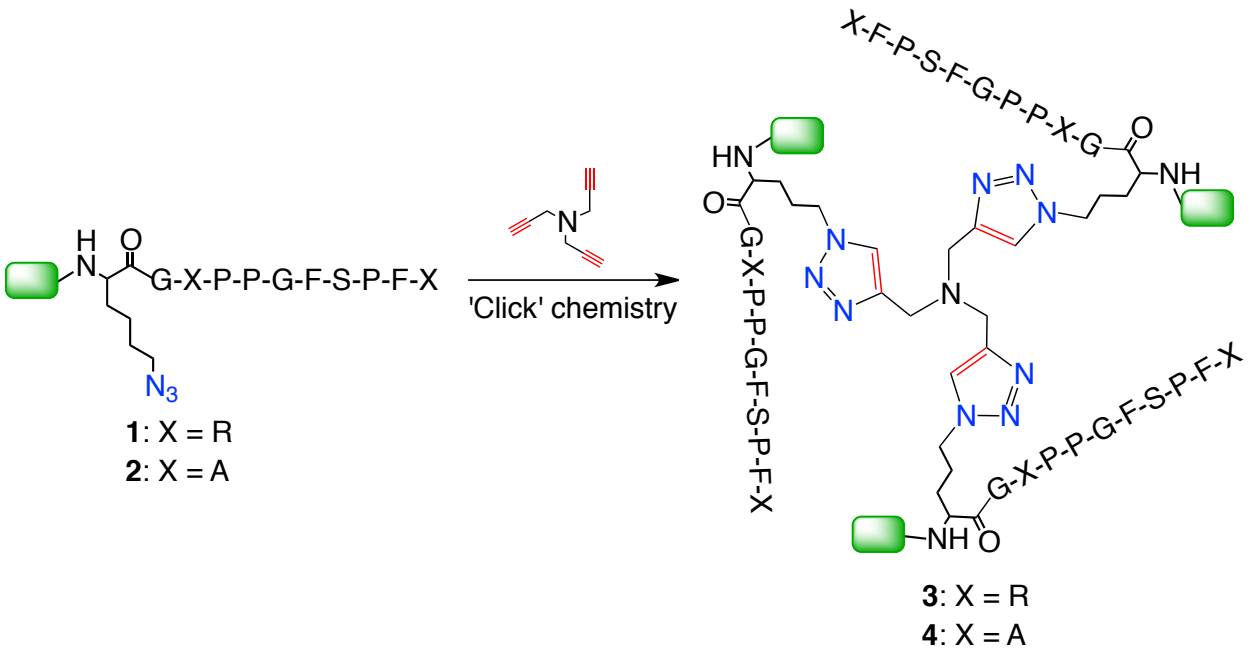

1: X = R
2: X = A

3: X = R
4: X = A

Typically, peptide **1** (8 mg, 4.2 μmol, 3.6 equiv.) was taken up in 150 μL MeOH that was purged with N_2 for at least 30 min. To this mixture was added tripropargylamine (0.16 mg, 1.2 μmol, 1 equiv.) in 50 μL MeOH, followed by the addition of Tris[(1-benzyl-1*H*-1,2,3-triazol-4-yl)methyl]amine (TBTA, 3.2 mg, 6 μmol, 6 equiv.) and Tetrakis (acetonitrile)copper(I) hexafluorophosphate ($[(CH_3CN)_4Cu]PF_6$, 13.4 mg, 36 μmol, 30 equiv.). To this mixture was added MeCN dropwise to bring everything into solution, and the reaction was allowed to proceed at room temperature with constant stirring for 20 h. The sample was quenched with 1 mL H_2O, frozen, and lyophilized to dryness. The dried crude product was re-suspended in 0.1 M EDTA, loaded on a 5 mg Sep-Pak C18 cartridge, and sequentially eluted with 5 mL of H2O, 1:1 H_2O/MeCN, and MeCN. The H_2O/MeCN fraction was concentrated to dryness, purified by reversed phase C18 HPLC, and lyophilized to yield peptide **3** (BKKG-tri). Peptide **4** (BKKG-R3AR11A) was prepared in the same manner as described for **1**. Both peptides were

characterized by high resolution ESI-TOF-MS because these multimeric constructs did not ionize well by MALDI-TOF-MS: BKKG-tri **3**: $[M+3H]^{3+}$ calculated for $C_{219}H_{309}N_{76}O_{48}^{3+}$, 4771.4; found, *m/z* 1590.8; $[M+4H]^{4+}$ calculated for $C_{219}H_{310}NaN_{76}O_{48}^{4+}$, 4772.4; found, *m/z* 1193.1; $[M+5H]^{5+}$calculated for $C_{219}H_{311}N_{76}O_{48}^{5+}$, 4773.4; found, *m*/z 954.9. BKKG-R3AR11A-tri **4**: $[M+2H]^{2+}$ calculated for $C_{201}H_{266}N_{58}O_{48}^{+}$, 4260.0; found, *m/z* 2130.2; $[M+3H]^{3+}$ calculated for $C_{201}H_{267}N_{58}O_{48}^{+}$, 4261.0; found, *m/z* 1420.5; $[M+4H]^{4+}$ calculated for $C_{201}H_{268}N_{58}O_{48}^{+}$, 4262.0; found, m/z 1065.6.

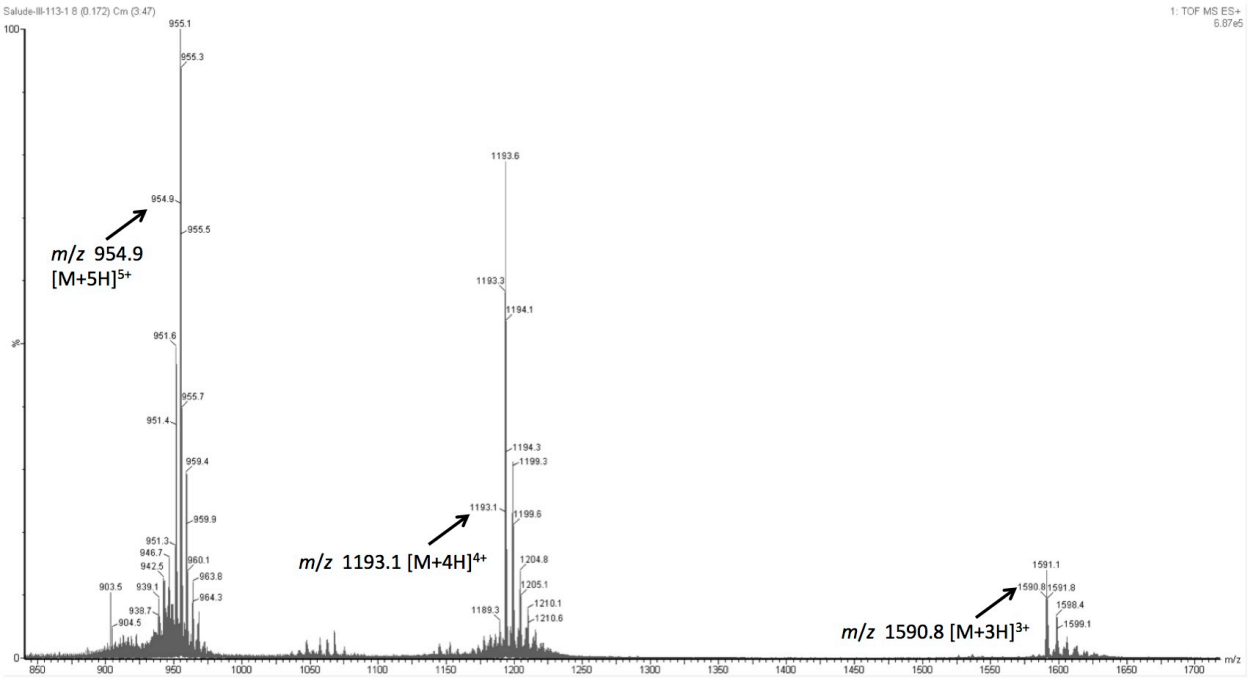

Figure S7. ESI-MS of BKKG-tri **3**.

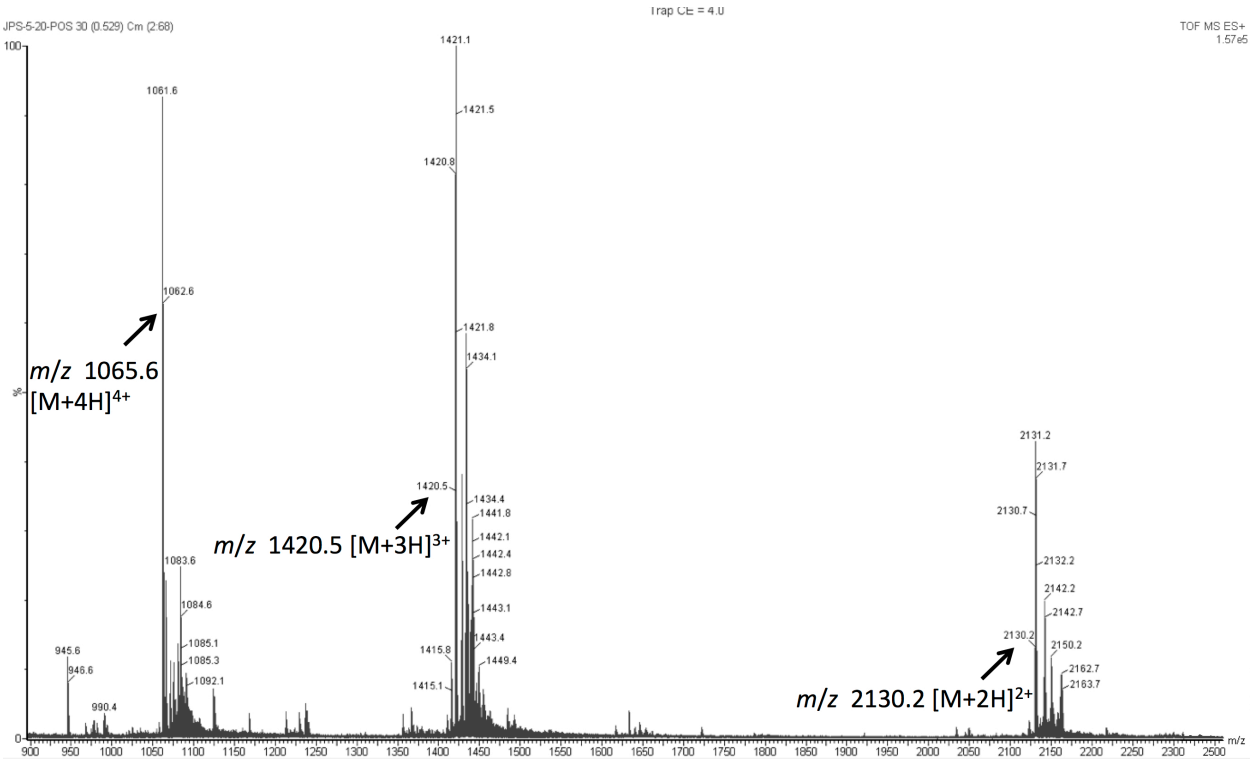

Figure S8. ESI-MS of BKKG-R3AR11A-tri **4**.

B. Studies with Synthetic Lipid Vesicles

B.1. Lipid Vesicle Preparation. Synthetic lipid vesicles were prepared as previously described[2] and were composed of the following:

Lipid Model 1 (LM1): 70% POPC, 15% POPE, 15% Cholesterol, 0% POPS

Lipid Model 2 (LM2): 60% POPC, 15% POPE, 15% Cholesterol, 10% POPS

Lipid Model 3 (LM3): 50% POPC, 15% POPE,15% Cholesterol, 20% POPS

where:

POPC = palmitoyl oleoyl phosphatidylcholine

POPE = palmitoyl oleoyl phosphatidylethanolamine

POPS = palmitoyl oleoyl phosphatidylserine.

Briefly, a lipid film was deposited on a glass vial by blowing down to dryness with Ar gas a $CHCl_3$ solution of the lipids (Avanti Polar Lipids, Alabaster, Alabama), followed by the removal

of residual organic solvent under vacuum for several hours. The lipid film was hydrated overnight at 4 ºC in PBS pH 7.4, the lipid suspension of multilamellar vesicles were subjected to five freeze-thaw cycles (except for extrusion through 400 nm pores), and followed by extrusion through polycarbonate membranes with pore diameters of 30, 100, and 400 nm to produce the desired vesicles using LiposoFast LF-50 (Avestin, Ottawa, Ontario). Representative samples from each unilamellar vesicles were taken and diluted with PBS to a lipid concentration of 10 – 20 μM and their sizes analyzed using Dynapro dynamic light scattering instrument (Wyatt Technology, Santa Barbara, California) that was calibrated using commercially available 50 nm polystyrene beads (Polysciences, Warrington, Pennsylvania). Figure S7 shows the representative sizes of the extruded liposomes. Aliquots of lipid vesicles were deposited on the surface of Formvar-carbon grids, air-dried, stained with 1% Uranyl acetate in water, and transmission electron microscope (TEM) images were recorded at x34,000 magnification using Philips CM10 TEM (Hillsboro, OR, USA), as shown in Figure S8.

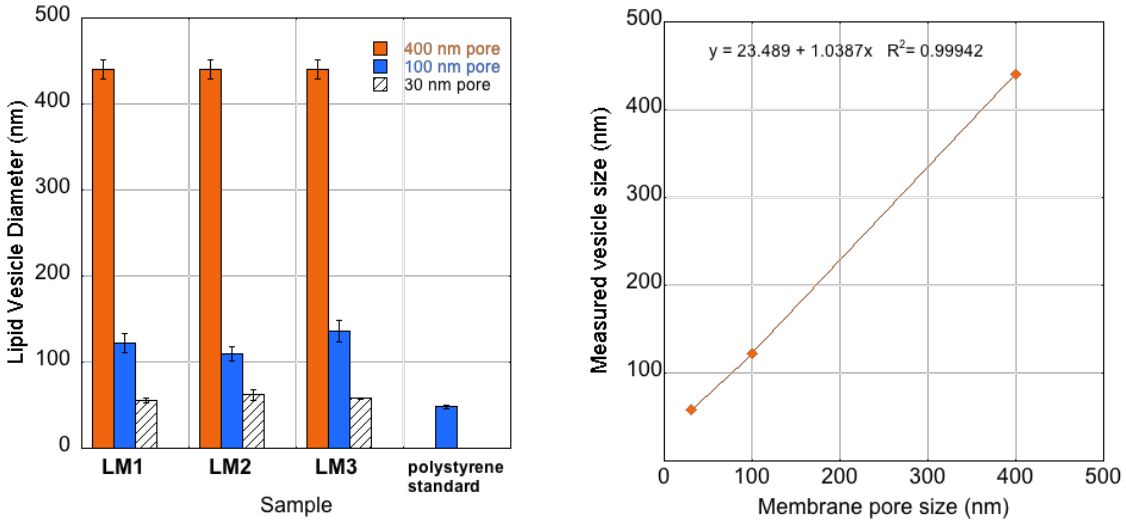

Figure S9. Dynamic light scattering (DLS) data for lipid vesicles. (a) Dynamic light scattering data showing the sizes of lipid vesicles made from LM1, LM2, and LM3 using polycarbonate membranes with pore sizes of 400, 100, and 30 nm to produce V_{454}, V_{116}, and V_{58}, respectively. b) Plot of membrane pore size versus lipid vesicle size showing a linear correlation.

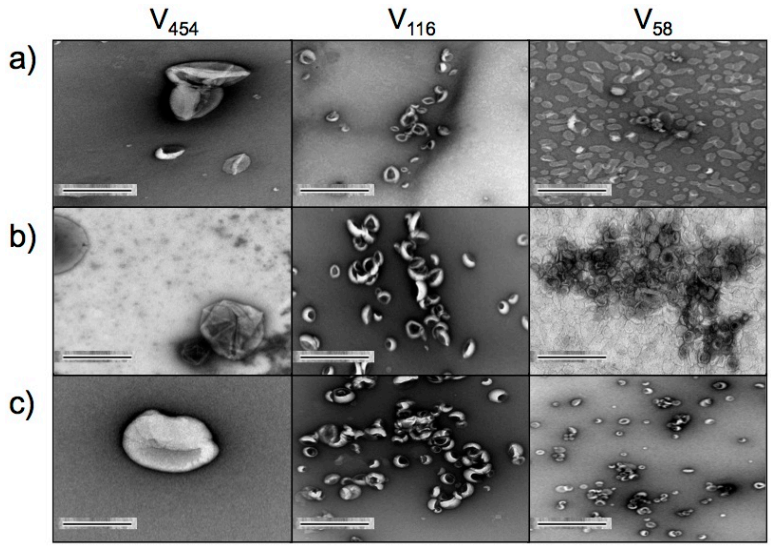

Figure S10. Transmission electron microscopy (TEM) images of liposomes. Negative stain transmission electron microscopic (TEM) images of untreated synthetic lipid vesicles. From left to right: Lipid vesicles V_{454}, V_{116}, and V_{58} extruded through 400, 100, and 30 nm pore sizes, respectively. The scale bar length is 0.40 μm at x34000 magnification.

B.2. Fluorescence Experiments. The peptide and lipid vesicle concentrations for fluorescence enhancement assays was optimized at 0.5 μM and 500 μM, respectively, previously reported.[3] Fluorescence enhancement measurements were recorded in triplicates by measuring the fluorescence emission spectra of 300 μL solutions of peptides **1** – **4** in PBS pH 7.4 at room temperature with λ_{ex} 480 and λ_{em} scan of 500-650 nm. Separate peptide-conjugate solutions were also prepared in the presence of 0.5 mM liposomes that were incubated at 4 ºC for two hours, and their fluorescence emission spectra recorded under identical conditions as above. As positive control, 0.20 μM of rat Syt1 C2AB (G374, residues 96-421)[4] was treated with Ca^{2+} (2.5 mM) and LM3 liposomes that were extruded through 30, 100, and 400 nm pores using λ_{ex} of 280 nm to excite Y364 in the membrane insertion loop 3.

For the anisotropy titrations, the peptides **1** - **4** (1 μM) were individually titrated with 2 mM of V_{454}, V_{116}, and V_{58} of LM1, LM2, and LM3. Anisotropy was monitored using the

Fluorolog-3 fluorometer. The excitation wavelength was set to λ_{ex} = 480 nm whereas the emission wavelength was set to λ_{em} = 545 nm. The voltage was set to 250 V throughout the experiment. Titrations were made to produce the [Total Lipid] on the x-axis versus the anisotropy values on the y-axis. The mixture was allowed to equilibrate after each titration. The following equation was used to quantify the dissociation constants as previously reported [5, 6]: $f_b = K_p[L]/(1 + K_P[L])$, where f_b expresses the fraction of peptide bound to lipids, K_p expresses the molar partition coefficient, and [L] expresses the lipid concentration. The equation was fitted to the anisotropy plot where the inverse of K_p correlates to the apparent dissociation constant, K_d.[5, 6]

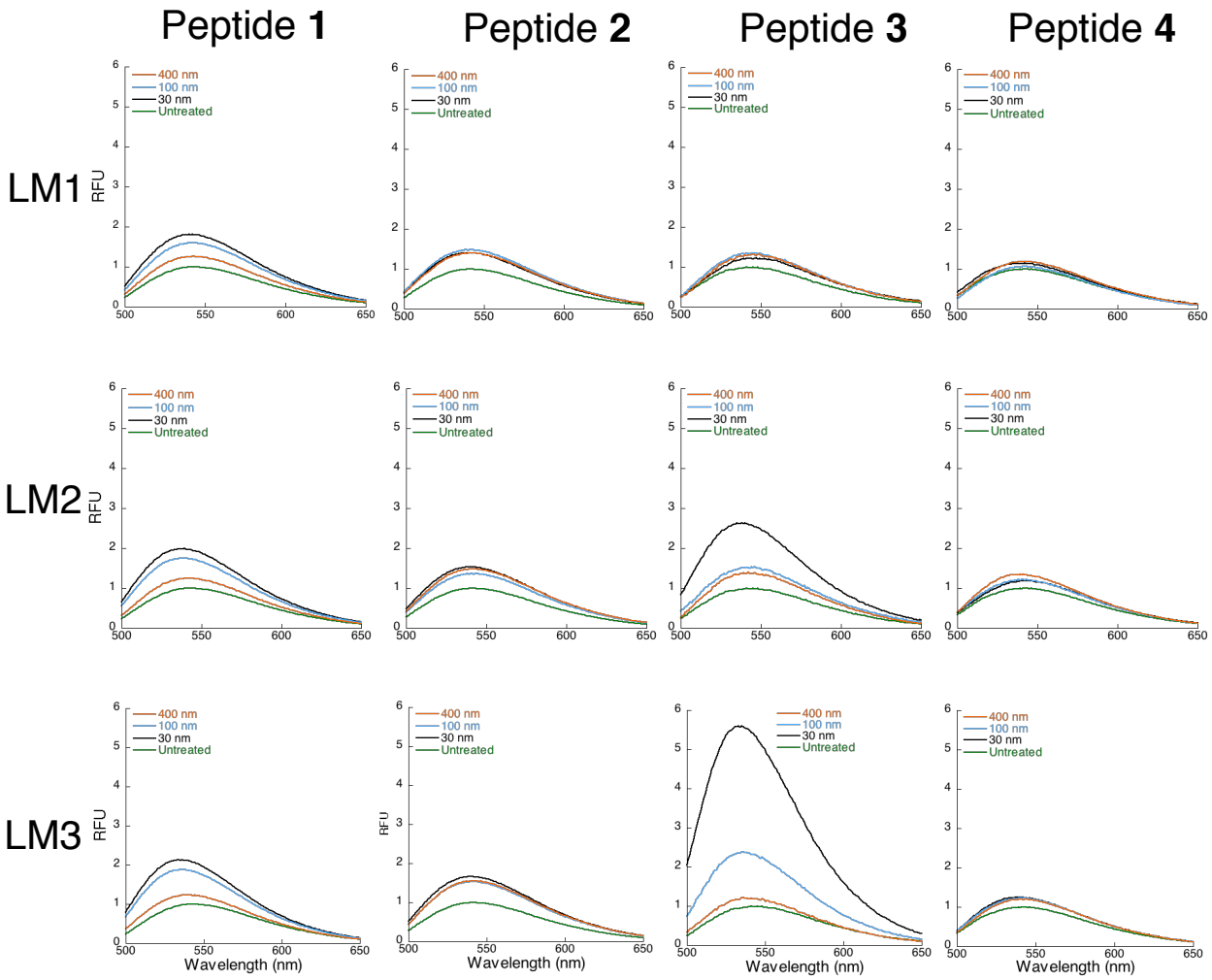

Figure S11. Fluorescence enhancement (FE) plots showing the interactions of peptides 1 - 4 with LM1, LM2, and LM3. Top Panel: FE profiles of peptides **1** – **4** with LM1. Middle Panel: FE profiles of peptides **1** – **4** with LM2. Bottom Panel: FE profiles of peptides **1** – **4** with LM3.

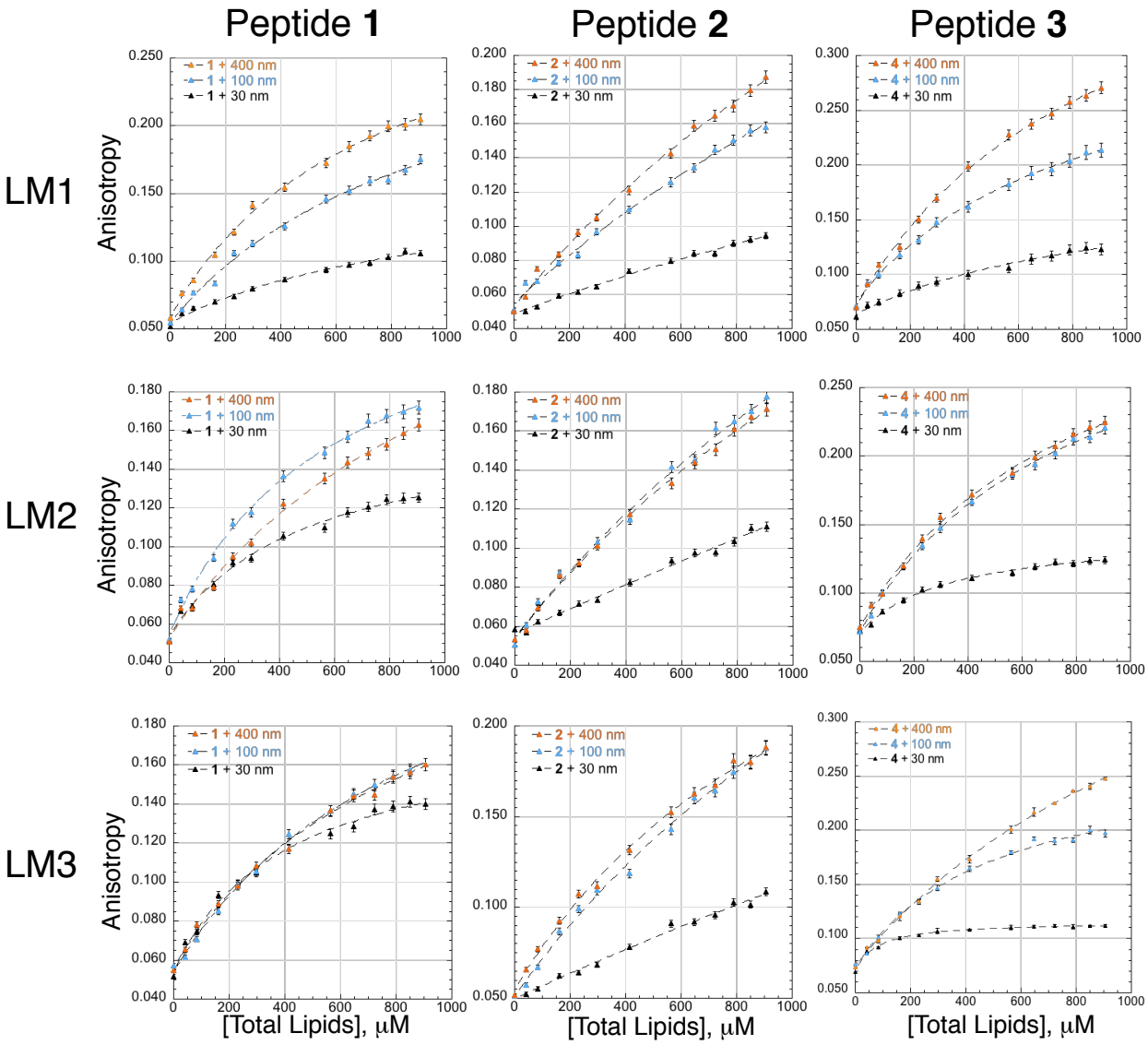

Figure S12. Fluorescence Anisotropy. Top Panel: Plots showing the binding saturation curves of peptides **1** – **3** with LM1. Middle Panel: Plots showing the binding saturation curves of peptides **1** – **3** with LM2. Bottom Panel: Plots showing the binding saturation curves of peptides **1** – **3** with LM3. The binding plots were fitted using a standard one-site saturation equation (*5*).

B.3. Circular Dichroism. Solutions of peptides **1** and **2** were prepared at 240 μM concentration in phosphate buffer, pH 7.4. 200 mL aliquots were taken and diluted with 200 μL buffer to produce 120 μM peptide solutions. Circular dichroism spectra were recorded using Chirascan spectrometer (Applied Photophysics, Surrey, UK) in a 1 mm path length quartz cuvette at 20 ºC using phosphate buffer, pH 7.4 as blank. Five scans from 190 to 260 nm with data points taken every 1.0 nm were obtained and averaged for each sample. For the LM3 treated peptides, the same steps were taken as above. However, 200 μL of 80 μM LM3 were used as diluent instead of the buffer.

C. Studies with Rat Exosomes

C.1. Isolation of Exosomes. Exosomes from rat models were prepared and characterized by ELISA as previously described.[3] The isolated exosomes were resuspended in PBS and this material is hereinafter referred to as Ex.

C.2. Transmission Electron Microscopy. Aliquots of plasma and Ex were deposited on the surface of Formvar-carbon grids, air-dried, stained with 1% Uranyl acetate in water, and transmission electron microscope (TEM) images (Figure S11) were recorded as described above using x25,000 magnification.

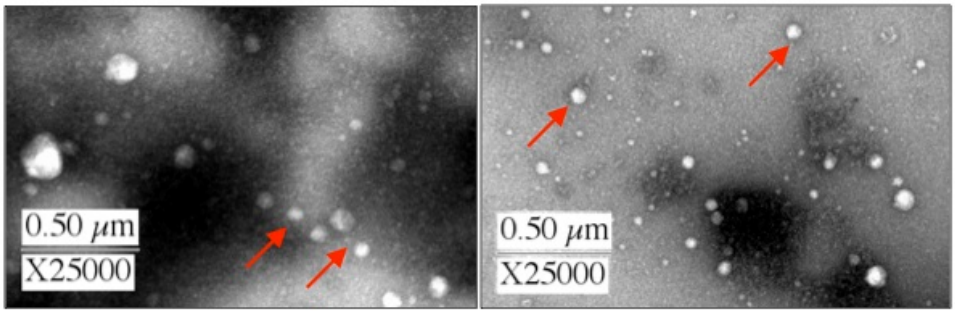

Figure S13. TEM images of exosomes. TEM images of untreated plasma (left) and purified exosomes (Ex, right) showing vesicles with d ≤ 100 nm. Arrows indicate ~50 nm exosomes.

C.3.

Vesicle Counting by Nanoparticle Tracking Analyses. Nanoparticle Tracking Analyses (NTA) were performed using NanoSight LM10-HS (NanoSight Ltd., Amesbury, UK) instrument equipped with a 532 nm laser. The instrument was calibrated using commercially available 50 nm polystyrene beads (Polysciences, Warrington, Pennsylvania). Aliquot of Ex, LM1, LM2, and LM3 V_{58} were taken and diluted with appropriate volumes of PBS, pH 7.4 to give a particle count between 1 – 8 x 10^8 mL^{-1}, following a previous work on nano-sized vesicles.[7] The particle count and the size distribution of the undiluted sample was back calculated to give the profile of the LM1, LM2, and LM3 in the original sample as shown in Fig. S12. This analysis showed that the final lipid vesicle concentration in the fluorescence enhancement assays (Sec. B.2 and Sec. C.4) for Ex, LM1, LM2, and LM3 corresponded to 6.51 x 10^{12}, 4.48 x 10^{12}, 5.60 x 10^{12}, and 4.70 x 10^{12} particles/mL, respectively.

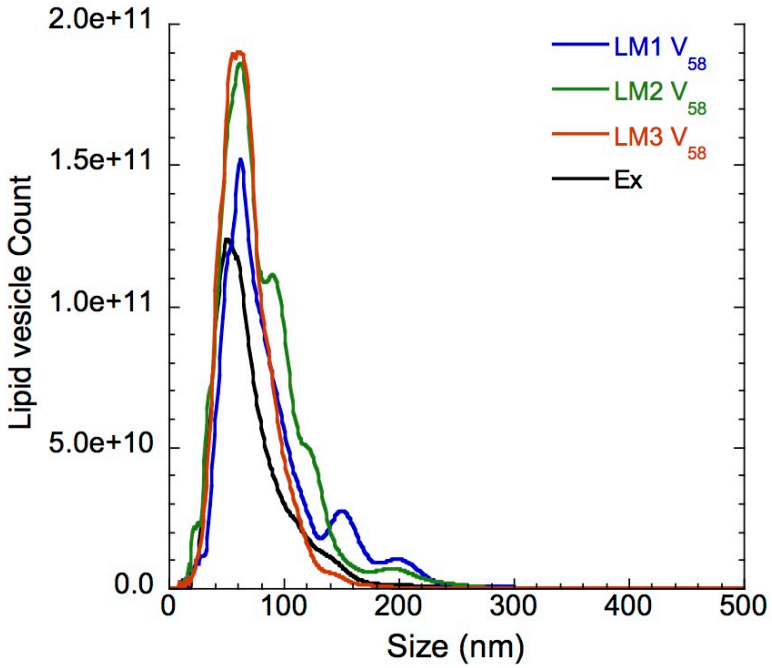

Figure S14. NTA Analysis. Profile of Ex and LM1, LM2, and LM3 V58 lipid vesicles used for fluorescence enhancement assays.

C.4. Fluorescence Experiments. Five microliters each of PBS, pH 7.4 solution of peptides **1** and **3** were added to 295 μL of Ex from Sec. C.1 and their fluorescence spectra recorded following the method described in Sec. B.2.

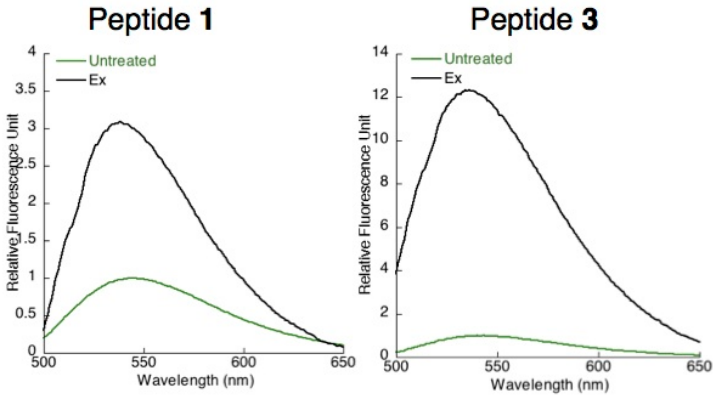

Figure S15. FE profiles of peptide and Ex interactions. Left Panel: FE profile of peptide **1** with Ex. Right Panel: FE profile of peptide **3** with Ex.

References for Supporting Information

1. A. K. Oyelere, P. C. Chen, L. P. Yao and N. Boguslavsky, *J. Org. Chem.*, 2006, **71**, 9791-9796.
2. L. A. Morton, J. P. Saludes and H. Yin, *J. Vis. Exp.*, 2012, **64**.
3. J. P. Saludes, L. A. Morton, N. Ghosh, L. Beninson, E. R. Chapman, M. Fleshner and H. Yin, *ACS Chem. Biol.*, 2012, **7**, 1629-1635.
4. E. F. Hui, C. P. Johnson, J. Yao, F. M. Dunning and E. R. Chapman, *Cell*, 2009, **138**, 709-721.
5. L. Rusu, A. Gambhir, S. McLaughlin and J. Radler, *Biophys. J.*, 2004, **87**, 1044-1053.
6. G. Vergeres and J. J. Ramsden, *Biochem. J.*, 1998, **330**, 5-11.
7. R. A. Dragovic, C. Gardiner, A. S. Brooks, D. S. Tannetta, D. J. P. Ferguson, P. Hole, B. Carr, C. W. G. Redman, A. L. Harris, P. J. Dobson, P. Harrison and I. L. Sargent, *Nanomedicine: NBM*, 2011, **7**, 780-788.